archives
of thermodynamics
Vol. **40**(2019), No. 1, 161–185
DOI: 10.24425/ather.2019.128296

Analysis of the reliability of photovoltaic-micro-wind based hybrid power system with battery storage for optimized electricity generation at Tlemcen, north west Algeria

MOHAMMED SALIM HADJIDJ*
NACEREDDINE BIBI-TRIKI
FAOUZI DIDI

Unit of Research on Materials and Renewable Energies, Department of Physics, Faculty of Sciences, Abou Bekr Belkaid University, BP 119-13000-Tlemcen, Algeria

Abstract This article considers designing of a renewable electrical power generation system for self-contained homes away from conventional grids. A model based on a technique for the analysis and evaluation of two solar and wind energy sources, electrochemical storage and charging of a housing area is introduced into a simulation and calculation program that aims to decide, based on the optimized results, on electrical energy production system coupled or separated from the two sources mentioned above that must be able to ensure a continuous energy balance at any time of the day. Such system is the most cost-effective among the systems found. The wind system adopted in the study is of the low starting speed that meets the criteria of low winds in the selected region under study unlike the adequate solar resource, which will lead to an examination of its feasibility and profitability to compensate for the inactivity of photovoltaic panels in periods of no sunlight. That is a system with fewer photovoltaic panels and storage batteries whereby these should return a full day of autonomy. Two configurations are selected and discussed. The first is composed of photovoltaic panels and storage batteries and the other includes the addition of a wind system in combination with the photovoltaic system with storage but at a higher investment cost than the first. Consequently, this result proves that is preferable to opt for a purely photovoltaic system supported by the

*Corresponding Author. Email: salimhadjidj14@gmail.com

storage in this type of site and invalidates the interest of adding micro wind turbines adapted to sites with low wind resources.

Keywords: Modeling; Optimization; Simulation; Photovoltaic system; Wind system; Hybrid photovoltaic-wind-storage system; Sizing; Optimization

Nomenclature

A	–	scale parameter, m/s
A_i	–	anisotropy index, $\left(=\frac{G_b}{G_0}\right)$
C_i	–	available battery capacity, Ah
E	–	energy, Wh
f	–	factor used to account for lightening the horizon $\left(=\sqrt{\frac{G_b}{G}}\right)$
	–	Weibull probability density function
	–	fraction of total power
G	–	global horizontal radiation on the surface of the Earth, kW/m^2
G_0	–	monthly mean daily extraterrestrial solar radiation
G_b	–	beam radiation, kW/m^2
G_d	–	scattered radiation, kW/m^2
G_{inc}	–	illumination junction in operating conditions
H	–	solar irradiation on an inclined plane, kW/m^2
K	–	shape factor
LSP	–	loss of power supply, W
S_{eol}	–	area swept by the wind turbine blade, m^2
N	–	power conditioning efficiency (= 0.8)
N_{bat}	–	total number of batteries
N_{eol}	–	total number of wind generator
N_{pv}	–	total number of photovoltaic panels
P_{bat}	–	input/output power of battery, W
P_{dd}	–	depth of battery discharge
P_{eol}	–	power output of wind generator, W
P_f	–	module fill factor (= 0.9)
P_{inv}	–	inverter input power
P_{load}	–	load demand
P_{pv}	–	power output of photocoltaic panel, W
P_{re}	–	total power transferred to battery bank, W
R_b	–	ratio of beam radiation on an inclined and horizontal surfaces
R_{pv}	–	performance of the photovoltaic generator
S_{eol}	–	total surface swepted by blades of wind generator, m^2
S_{pv}	–	total surface of the photovoltaic generator, m^2
T	–	time period
t	–	hours of the day, h
Δt	–	simulation time step, h
T_a	–	average ambient daily temperature, °C
T_c	–	daily temperature of average cell, °C

T_{NOCT}	–	nominal operating cell temperature, °C
T_{STC}	–	temperature of photovoltaic cell in standard test conditions (= 25 °C)
V_{bus}	–	direct bus voltage, V
V	–	wind speed, m/s
WE	–	wasted energy, W

Greek symbols

β	–	surface slope
γ	–	considering the variation in performance of the photovoltaic module according to the temperature, which is take at (0.0045/°C)
Δt	–	time step, h
η_{bat}	–	battery efficiency
η_{inv}	–	inverter efficiency (= 93%)
η_r	–	reference performance of the photovoltaic generator
ρ	–	air density (= 1.225 kg/m^3)
ρ_g	–	ground reflectance (albedo)

1 Introduction

Economic growth requires increasing demand for electrical energy to ensure the development and comfort of human life. The exploitation of fossil fuels has a negative impact on the environment and hence the need for a healthy and sustainable energy transition, such as the exploitation of renewable energy potential, particularly for regions remote from conventional electricity networks. The daily average solar energy received over most of the northern part of the Algerian territory is approximately 5 kWh which has a low to medium wind resource. The latter represents a minor wind potential in some sites, which could also be exploited by means of micro wind turbines with low starting speed.

Tlemcen, a city located in northern Algeria, is a home to sites far from conventional electricity networks where a number of research studies have previously been conducted on the operation of photovoltaic and/or wind energy systems. However, no studies have been carried out on sites with low or medium wind potential for energy production systems using micro wind turbines.

The decrease of absence of yield of photovoltaic panels in periods of low or no sunlight, particularly at night, causes a handicap resulting in the oversizing of a possible battery-powered photovoltaic system. In this case, the study will determine if a micro wind turbine system has a good energy and economic impact that favours its hybrid integration with the photovoltaic system and electrochemical storage mentioned above.

The main objective of this study is to determine whether it is more efficient from the energy point of view and economically viable to adopt a photovoltaic system with storage or to opt for the same smaller system by integrating a micro-wind turbine system. The focus is on identifying the optimal configurations of systems aimed at providing a continuous and constant energy balance to an autonomous housing either consumed directly or stored in batteries. The scientific interest in this study is based on a judicious approach and choice of the discreet model and its application to photovoltaic-micro-wind hybrid systems, which is introduced into a simulation and calculation program that performs an hourly simulation of the energy balance between the total daily load of the living residence and the other components of the system during the reference year 2018.

In the end, two optimal configurations are chosen. The first includes a photovoltaic system assisted by electrochemical storage generating a total cost (without installation cost) of 4125 EUR and the second includes the addition of a micro wind turbine system to a system with fewer photovoltaic panels and batteries. The cost of that installation amounts to 5735 EUR.

It can therefore be noted that the exploitation of the low wind potential by the use of micro wind turbine system is not very reliable even in a site with a low wind resource similar to our case study and it would be more advantageous to rely on the use of pure photovoltaic system assisted by storage batteries that offer better reliability and energy efficiency as well as a greater economic profitability.

2 Site description and assessment of solar and wind resources and load required

2.1 Implementation site

The chosen site is located in Tlemcen in a region of Zenâta in Algeria. The characteristics of the site is displayed in the Tab. 1:

Table 1: Characteristics of the Zenâta site [2].

Site	Latitude	Longitude	Altitude	Albédo
Tlemcen	35.02 °N	1.18 °E	247 m	0.20

2.2 Solar and wind resource assessment

The local resource data (solar irradiation and wind speed) is fundamental to be known with precision for the selected region. This study is based on a source of daily data from the two sources of solar and wind energy measured at a height of ten meters above the ground level related to twelve months and the whole year for ten consecutive years (2000–2010). The data were obtained from the Metar/Synop meteorological station in Tlemcen Zenâta [3].

2.2.1 Solar resource

Figure 1 shows the monthly average of each year of the solar radiation index for the Tlemcen region. The solar radiation in Tlemcen reaches its minimum of 2.3 kWh/m^3/day in December and its maximum of 7.5 kWh/m^2/day in June. The annual average is 4.8 kWh/m^2/day.

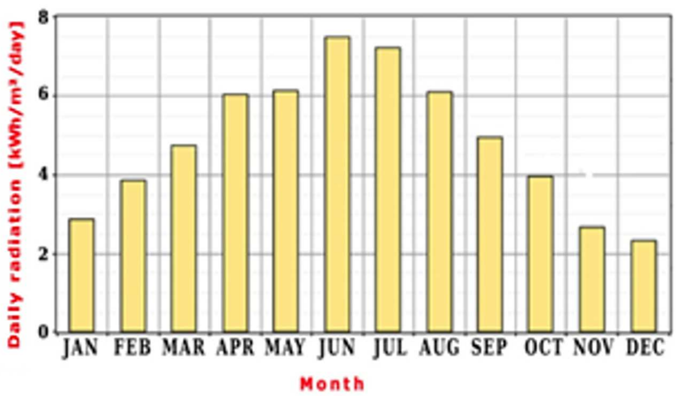

Figure 1: Monthly sun radiation for the Tlemcen site.

2.2.2 Wind resource

Figure 2 shows the annual average wind speeds in the Tlemcen region. Wind speeds are considered relatively low throughout the year. January is the windiest month with the wind speed of 3.2 m/s and October is the least windy month of the year with a speed of 1.3 m/s. The annual average wind speed at the Tlemcen site is 2.1 m/s for the period studied. Solar radiation and wind speeds are considered appropriate for the proper functioning of the energy system.

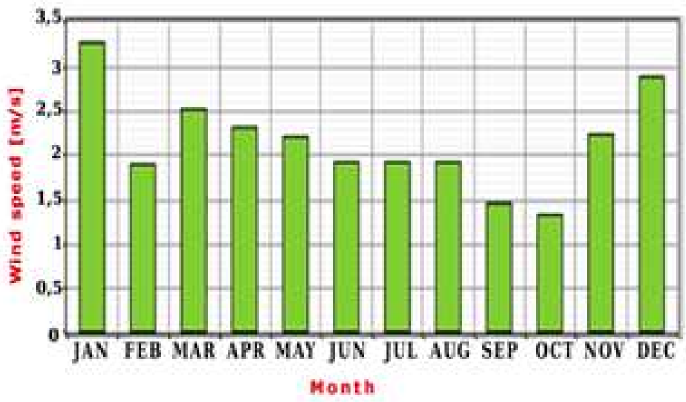

Figure 2: Monthly wind speeds at the Tlemcen site.

2.2.3 Temperature

Table 2 displays the monthly average of each year's temperature in the Tlemcen region. The monthly temperature reaches its minimum in January and is estimated at 6.27 °C whereas its maximum of 28.9 °C is found in July and the annual average is 17 °C. These temperatures will not affect the proper operation of the converters in the photovoltaic installation or wind turbines.

2.3 Characteristics of the chosen apartment and its energy balance

The apartment chosen for the study is of the type not connected to the conventional energy distribution network and equipped with all the appliances to provide comfort to the occupants. In addition, it is permanently occupied throughout the year and domestic equipment operates under a standard voltage of 220 V/50 Hz. Daily consumption is assumed to be constant during the first nine months of the year (September–May) at around 3.260 kWh per day and another constant value during the summer season (June, July, and August) estimated at 9.150 kWh per day (see Tab. 2)[4].

Figure 3 represents the total consumption of the apartment in a single

Table 2: Average monthly temperature.

Month	Temperature [°C]
Jan.	6.27
Feb.	8.23
March	11.6
Apr.	14.8
May	19.9
June	25.4
July	28.9
Aug.	28.0
Sep	23.1
Oct.	17.6
Nov.	11.7
Dec.	7.6
Annual average	17.0

typical day during the winter season (3.260 kWh) shared over 24 hours. Figure 4 represents the total consumption of the apartment in a single day during the summer season (June–August): 9.150 kWh, shared over 24 hours. Table 3 shows the estimate of the daily energy needs of the apartment in watt-hours.

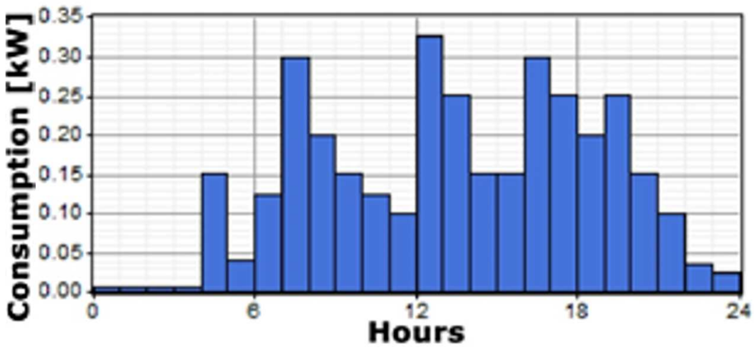

Figure 3: Daily profile (winter season).

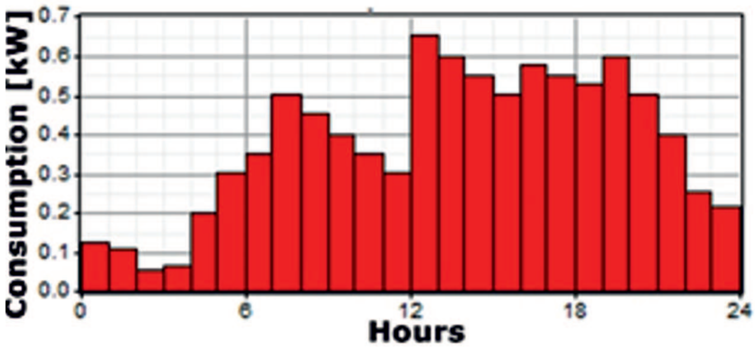

Figure 4: Daily profile (summer season).

Table 3: Assessment of daily energy needs of apartment.

		Power [W]	Duration of use [h]	Daily consumption [Wh]
Lighting	adults' room	11	4	44
	children's room	22	5	110
	living room	22	6	132
	corridor	22	2	44
	bathroom	22	2	44
	toilets	11	1	11
	kitchen	11	7	77
Appliances	refrigerator	120	8 (winter), 12 (summer)	96 (winter), 1440 (summer)
	television LCD	72	5.5	397.26
	air conditioner	1100	0 (winter), 6 (summer)	0 (winter), 6600 (summer)
	Others	100	2	250
Total lighting of apartment				3260/9150

3 Methodology

The essential step in the dimensioning of energy production system is the determination of its optimal size which depends essentially on the climatic data of the site and the characteristics of the parameters included in this system. This part deals with the models used in this study to determine the optimal size of the electrical energy production system to meet the electrical needs of the residence.

3.1 Incident global radiation and energy produced by the photovoltaic generator

Incident global radiation, G_T, on a photovoltaic panel is calculated according to the HDKR (Hay, Davies, Klucher, Reindl) model [5]

$$G_T = (G_b + G_d A_i)R_b + G_d(1 - A_i)\left(\frac{1+\cos\beta}{2}\right)\left[1 + f\sin^3\left(\frac{\beta}{2}\right)\right] + G\rho_g\left(\frac{1-\cos\beta}{2}\right), \quad (1)$$

where A_i is the anisotropy index, which is a function of transmittance of the atmosphere for beam radiation and defined as $A_i = \frac{G_b}{G_0}$ (G_0 is monthly mean daily extraterrestrial solar radiation), and f is the factor used to account for lightening the horizon, defined as $f = \sqrt{\frac{G_b}{G}}$.

The power produced by a photovoltaic panel, P_{pv}, in a day i $(1 \le i \le 365)$ and at hour t $(1 \le t \le 24)$ is estimated from the data of the global irradiation on inclined plane, ambient temperature and the manufacturer's data of the photovoltaic module used. It is given by [6]

$$P_{pv,i}(t) = R_{pv}\, S_{pv}\, P_f\, H\, N\,, \quad (2)$$

where S_{pv} is the total surface of the photovoltaic generator, P_f is the module fill factor, H is solar irradiation on the inclined plane, and N is the power conditioning efficiency.

The performance of the photovoltaic generator is represented by the following equations:

$$R_{pv} = \eta_r\{1 - \gamma(T_c - T_{STC})\}\,, \quad (3)$$

$$T_c = T_a + G_{inc}\left(\frac{T_{NOCT} - 20}{800}\right). \quad (4)$$

3.2 Wind speed distribution and energy produced by the wind generator

The Weibull probability density function $(f(V))$ is used to characterize the distribution of wind frequencies during the period studied and is defined by [7]

$$f(V) = \left(\frac{K}{A}\right)\left(\frac{V}{A}\right)^{K-1} \exp\left[\left(\frac{V}{A}\right)^{K}\right] , \tag{5}$$

where A and K are the scale and shape parameters, respectively (having same units as wind speed), and V is the wind speed. Wind speeds can be calculated based on Weibull K and A parameters as shown below [8]

$$V = A\Gamma\left(1 + \frac{1}{K}\right) . \tag{6}$$

The wind density power at hour t $(1 \leq t \leq 24)$ of a day i $(1 \leq i \leq 365)$ of a site based on the probability density function can be expressed as follows [9,10]:

$$P_{eol,i}(t) = \frac{1}{2} S_{eol} \rho V^3 \Gamma\left(1 + \frac{3}{K}\right) , \tag{7}$$

where S_{eol} is the surface swepted by the wind generator blades.

Once the wind density power is given, the energy produced by a wind generator, E_{eol}, for a desired period can be calculated by [9,10]

$$\frac{E_{eol}}{S_{eol}} = \frac{1}{2} \rho V^3 \Gamma\left(1 + \frac{3}{K}\right) T , \tag{8}$$

where T is the time period.

3.3 Battery size

The total power, $P_{re,i}$, transferred to the battery bank from the photovoltaic and wind generator power sources during day i $(1 \leq i \leq 365)$ and at hour t $(1 \leq t \leq 24)$, is calculated as follows:

$$P_{re,i}(t) = N_{eol} P_{eol,i}(t) + N_{pv} P_{pv,i}(t) , \tag{9}$$

where N_{pv} is the total number of photovoltaic panels, N_{eol} is the total number of wind turbine generator. Depending on the photovoltaic and wind generator production and the load power requirements, P_{load}, the battery state of charge is accumulated during the dimulation period as follows [11]:

$$C_i(t) = C_i(t-1) + \eta_{bat}(P_{bat,i}(t)/V_{bus})\Delta t , \tag{10}$$

where $C_i(t), C_i(t-1)$ is the available battery capacity at hour t and $t-1$, respectively, of a day i, $\eta_{bat} = 80\%$ is the battery round-trip efficiency during charging and $\eta_{bat} = 100\%$ during discharging, V_{bus} is the DC bus voltage, $P_{bat,i}(t)$ is the battery input/output power ($P_{bat,i}(t) < 0$ during discharging and $P_{bat,i}(t) > 0$ during charging) and Δt is the simulation time step, set to $\Delta t = 1$ h.

So, the state of charge, SOC_{bat}, is deduced from the battery power and efficiency, η_{bat}, [12]

$$SOC_{bat} = \int (P_{bat,charging} \times \eta_{bat} - P_{bat,discharging})dt \,, \tag{11}$$

where $P_{bat,charging}$ and $P_{bat,discharging}$, the battery input/output power, respectively. The minimum permissible battery capacity, C_{min}, during discharging is fixed at a depth of 50% from its nominal capacity, C_{max}. The battery bank nominal capacity, C_n, is related with the total number of batteries, N_{bat}, multiplied by the nominal capacity of each battery, C_{max}, devided by the number of series connected batteries.

3.4 Power management strategy

The power difference, $P_{net,i}(t)$, between the generation sources and the load demand, $P_{load,i}(t)$, is calculated as

$$P_{net,i}(t) = P_{pv,i}(t) + P_{eol,i}(t) - P_{load,i}(t) \,. \tag{12}$$

A governing control strategy is adopted, where at any time, any excess micro-wind and photovoltaic generated power ($P_{net} > 0$) is supplied to the battery. Therefore the power balance equation given in formula (12) can be written as

$$P_{pv,i}(t) + P_{eol,i}(t) = P_{load,i}(t) + P_{bat,discharging} \,. \tag{13}$$

When there is a defect in power generation ($P_{net} < 0$), the battery begins to produce energy for the load. Therefore, the power balance equation for this situation can be written as

$$P_{pv,i}(t) + P_{eol,i}(t) + P_{bat,discharging} = P_{load,i}(t) \,. \tag{14}$$

3.5 Modeling of system reliability

Several approaches are used to achieve the optimal configurations of hybrid systems in terms of technical analysis. In this study, the technical sizing model is developed according to the concept of the loss of power supply probability (LPSP) to evaluate the reliability of hybrid systems [13]. The methodology used can be summarized in the following steps:

The total power, $P_{tot,i}(t)$, generated by the micro wind photovoltaic generator at time t is calculated as follows:

$$P_{tot,i}(t) = P_{eol,i}(t) + P_{pv,i}(t) . \tag{15}$$

The total power is divided into two parts. If the fraction of $P_{tot,i}$ given by the photovoltaic system is f, then the complementary that is $(1 - f)$ of the, $P_{tot,i}$, must be satisfied by the wind system. The limit values of f correspond to systems without support from other installations. Hence, $f = 1$ corresponds to a 100% use of the photovoltaic system and $f = 0$ represents 100% of the wind system. So the previous Eq. (15) becomes

$$P_{tot,i,f}(t) = fP_{pv,i}(t) + (1 - f)P_{eol,i}(t) . \tag{16}$$

Then, the inverter input power, $P_{inv}(t)$, is calculated using the corresponding load power requirements, as follows:

$$P_{inv,i}(t) = \frac{P_{load,i}(t)}{\eta_{inv}} , \tag{17}$$

where $P_{load,i}(t)$ is the power consumed by the load at hour t, and η_{inv} is the inverter efficiency (93% in this study).

Three states may be appearing:

I. The total power generated by the micro wind turbine and photovoltaic cell is greater than the power needed by the load, P_{inv}. In this case, the energy surplus is stored in the batteries and the new storage capacity is calculated using Eq. (10) until the full capacity is obtained.

II. The total micro wind and photovoltaic power is less than the power needed by the load, P_{inv}, the energy deficit is covered by the storage and a new battery capacity is calculated using (Eq. (10)).

III. In case of inverter input and total power equality, the storage capacity remains unchanged.

In case I, when the batteries capacity reaches a maximum value, $C_{bat,max}$, the control system stops the charging process. The wasted energy, defined as the energy produced and not used by the system, for a hour t is calculated as follows:

$$\mathrm{WE}_i(t) = P_{tot,i}(t)\Delta t - \left\{ \frac{P_{load,i}(t)}{\eta_{inv}} \Delta t + \left[\frac{C_{n,\max} - C_{bat,i}(t-1)}{\eta_{bat}} \right] \right\} , \quad (18)$$

where Δt is the step of time used in the calculations (in this study $\Delta t =$ 1 h).

In case II, if the batteries capacity decreases to their minimum level, $C_{\min}$, the control system disconnects the load and the energy deficit, loss of power supply (LPS) for a time t can be expressed as follows [14]:

$$\mathrm{LPS}_i(t) = P_{load,i}(t)\Delta t - \{ [P_{tot,i,f}(t)] \Delta t + C_{bat,i}(t-1) - C_{min} \} \eta_{inv} \ . \quad (19)$$

The loss of power supply probability, for a considered period, T, can be defined as the ratio of all the LPS(t) values over the total load required during that period. The LPSP technique is considered as technical implemented criteria for sizing a hybrid micro-wind/photovoltaic system employing a battery bank. The technical model for hybrid system sizing is developed according to the LPSP technique [15]:

$$\mathrm{LPSP} = \frac{\sum_{t=1}^{T} \mathrm{LPS}_i(t)}{\sum_{t=1}^{T} P_{load,i}(t)\Delta t} \ . \quad (20)$$

3.6 Simulation and optimization

The reliability study model is introduced according to the algorithm of the calculation program. This program models the performance of several system configurations every hour of the year to determine its technical feasibility. The simulation process determines how a particular system configuration, a combination of system components of specific sizes, and an operating strategy that defines how those components work together, would behave in a given setting over a long period of time.

The optimization process simulates many different system configurations in search of the one that satisfies the load of the residence at the lowest cost. Optimization determines the optimal value of the variables over which the system designer has a control such as the mix of components that make up the system and the size or quantity of each.

4 Description of the system

The studied system contains photovoltaic panels connected in the direct current (DC) bus and storage batteries. Each storage battery is connected in series with the 120 V DC bus. A converter is used to convert the energy produced from photovoltaic panels, wind turbines, and energy stored in batteries into alternating current (AC). The energy produced by the system is supplied to the apartment. The energy not consumed after serving the charge is stored in batteries.

The photovoltaic system produces a direct voltage which is stored in the battery after passing through a charge controller of the photovoltaic system. The wind turbine produces alternating current that is converted to direct current and stored in the battery. A discharge load is also connected to the battery to deflect the excess charge when the battery is fully charged.

The diagram that groups each possible component of the system is illustrated in Fig. 5 [16]. The technical specifications of the main components of the energy system are given in Tab. 4 [16,17].

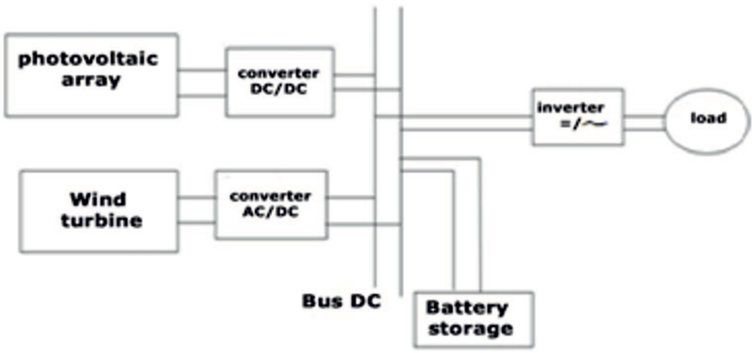

Figure 5: Flow diagram of the system.

5 Results and discussion

This part shows the influence of the characteristics of solar and wind energy resources on the sizing and profitability of an electrical energy production

Table 4: Technical details of the system.

Parameters	Values	Parameters	Values
photovoltaic panels	price: 65 EUR/panel	battery	price: 305 EUR/battery
nominal capacity [kW]	0.05	nominal voltage [V]	12
panel performance [%]	13	capacity [Ah]	230
voltage MPP [V]	18	maximum voltage [V]	14.4
intensity MPP [A]	2.78	starting current [A]	1150
short-circuit current [A]	3.16	charge voltage [%]	10
open-circuit voltage [V]	22.2	series-connected batteries	10
warranty [years]	10	life at 50% of discharge (cycle)	200
size (length/width/height) [mm]	630 × 545 × 25	size (length/width/ height)[mm]	518 × 276 × 242
weight [kg]	4	weight [kg]	56.75
life time (years)	20	warranty [years]	1
wind turbine	price: 2000 RUR/ turbine	convertor	prix: 1000 EUR/ convertor
rated capacity (W)	1000	maximum power [kW]	1210
maximum power [W]	1500	maximum voltage [V]	400
start speed [m/s]	2	voltage range PV, MPPT [V]	139–320
nominal speed [m/s]	10	max input current [A]	10
stop speed [m/s]	55	nominal power [kW]	1000
wind turbine efficiency [%]	96	output current [A]	5.6
noise level [dB]	45	nominal voltage range [V]	220–240/180–260
warranty [years]	5	frequency range network [Hz]	50–60
life time [years]	25	maximum efficiency [%]	93
weight [kg]	78	size (length/width/ height) [mm]	434 × 295 × 214
rotor length [m]	2.8	weight [kg]	22
rotor width [m]	2	noise level [dB]	39

MPP – maximum power point, MPPT – maximum power point tracking system. After entering the necessary data into the calculation program, it will run several simulations by modifying the parameters and determining the optimal solutions. The result of the simulation shows the most feasible configuration of the energy system as well as the energy production of each source. The results obtained from the recovered photovoltaic energy are illustrated in Fig. 6, which shows the variation profile of the recovered photovoltaic solar energy. Two maximum values are distinguished: the 110th day the recovered energy reaches 6.87 kWh and 6.80 kWh the 237th day.

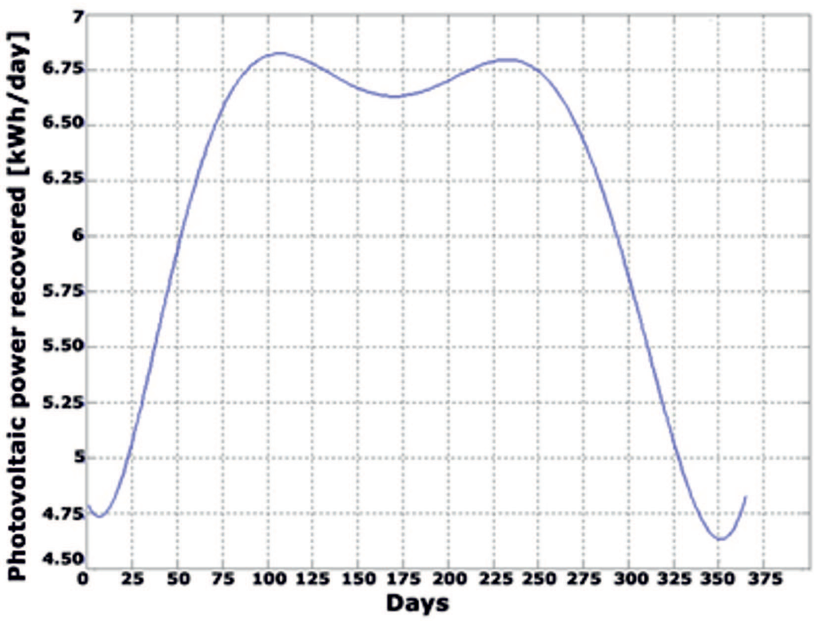

Figure 6: Solar photovoltaic energy received in the site on an inclined plane.

Wind energy recovered in relation to wind speeds for the Tlemcen region is shown in Fig. 7, which shows that January and December are the most profitable months of the year; the recovered wind energy reaches the value of 14.2 kWh per day. For the rest of the year, the energy is very low, which leads this region to use more photovoltaic rather than wind electricity. The wind rose and the wind speed frequency distribution were evaluated with respect to the entire year to determine if the wind is blowing in one direction throughout the year at a respective intensity. The annual results are shown in Fig. 8.

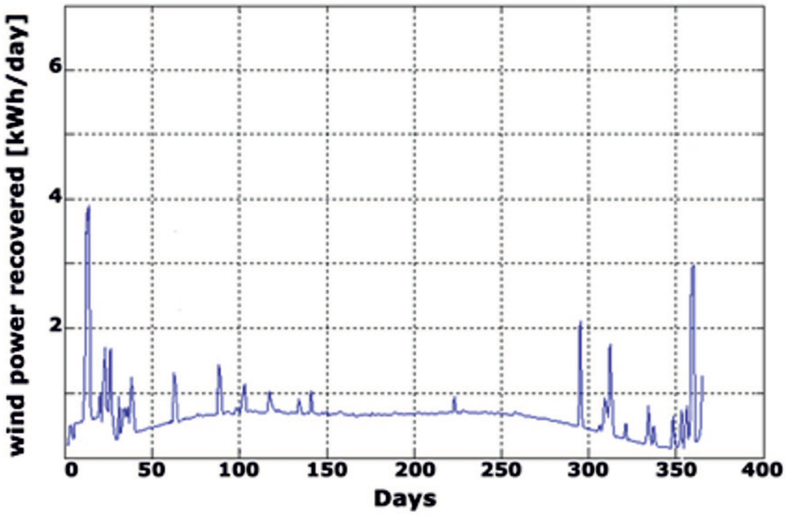

Figure 7: Daily wind energy collected in Tlemcen.

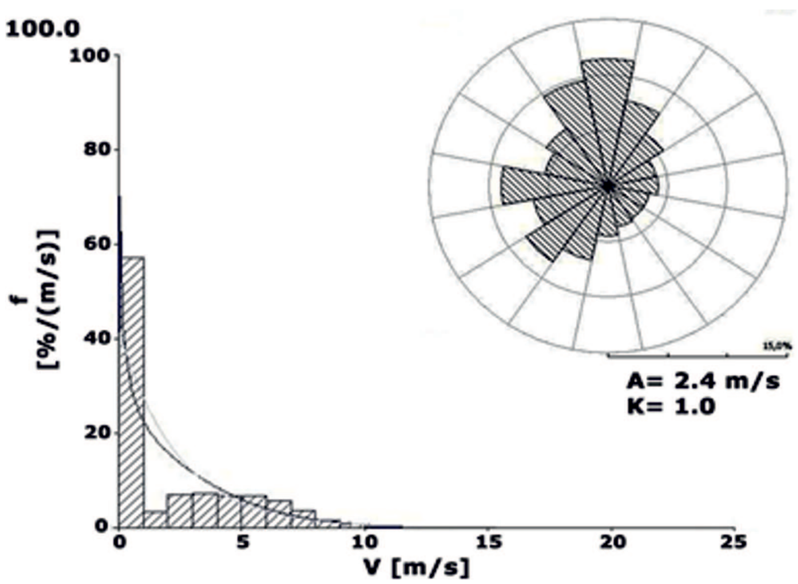

Figure 8: Wind speeds frequencies according to the Weibull distribution ans diagram of the wind rose at 10 m height.

The final value of the K and A parameters obtained are 1.00 and 2.42 m/s, respectively. The value of K is estimated at 1 m/s. Such low wind density is not conducive to the continuous operation of the wind system through out the entire day. Therefore, Tlemcen presents very low conditions in terms of wind resource. Concerning the wind rose diagram, it is notable that the prevailing wind directions come from the north side of Tlemcen.

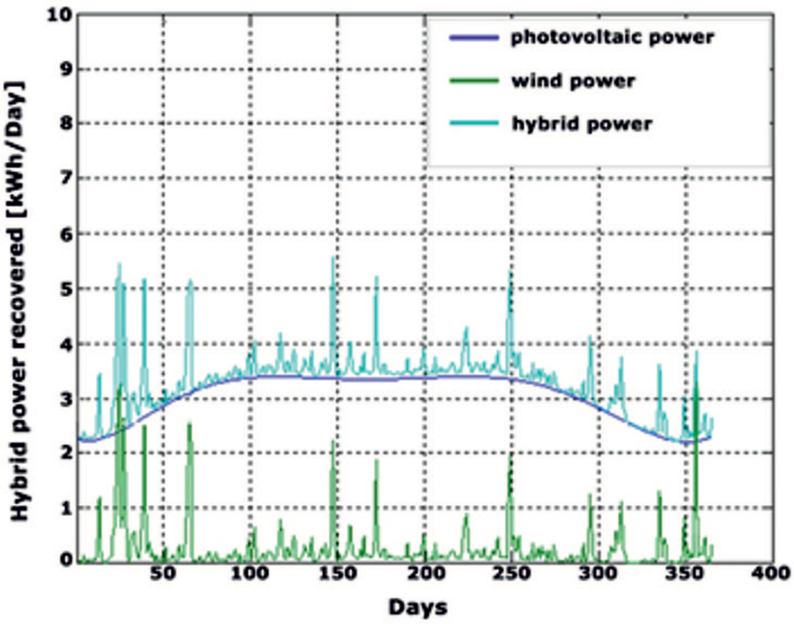

Figure 9: Hybrid energy (photovoltaic – wind) received.

The hybrid energy received for the Tlemcen region is shown in Fig. 9, which is interpreted over the following periods: The first period: from the first day to the 90th day, the apartment's load is fixed at 3.26 kWh/day (see Tab. 3). This winter period has 8 days in deficit which are: 1, 3, 5, 8, 10, 12, 15, and 16 days. This gives a day of autonomy since the days are not successive, so the storage in the batteries is introduced to cover the charge of the apartment. The second period: from 91st day to 274th day, the apartment's load is fixed at 9.15 kWh/day. This summer period does not include deficit days; the system works normally without batteries, the energy produced is fairly constant in this period and reaches the maximum value of 5.6 kWh/day. The third period: from the 275th day until the end of the year, the load of the apartment is fixed at 3.26 kWh/day. This winter period has other days in deficit which are: 235, 237, 239, and 242 days, that gives one day of autonomy.

Because the required load is constant for each period, the results show that the most unfavorable month in a year is the month with the lowest solar irradiation to wind speed ratio. According to the results, the most unfavorable month is December.

5.1 Calculating the number of batteries

The number of days of autonomy is estimated at one day (24 hours). The daily energy demand during this day is set at 3260 Ah. The storage system will compensate for the interruption of the power generation system. The electricity that comes out of the batteries does not reach the electrical appliances entirely: a part is lost in the wires and during the DC-AC conversion by the converter, the amount of energy to be restored is 3.95 kWh. For the batteries to have a longer life a maximum depth of discharge of 50% is set, the capacity of the storage system should be 7.91 kWh; this induces the necessity of having three storage batteries during this deficit day.

The calculation program finds the best configurations of the power generation system that will generate enough or all energy for the apartment. The results of these configurations are shown in Tab. 5.

Table 5: Optimum configurations.

Parameters	Optimum Configurations	
	Configuration A	Configuration B
photovoltaic system [kW]	1.7	1.4
number of panels PV	34	28
number of wind turbines	0	1
number of batteries	3	3
number of convertors	1	1
total cost [EUR}	4125	5735

Table 5 displays two best selected configurations. Configuration A contains a purely photovoltaic system with a power of 1.7 kW and consists of

34 photovoltaic panels, 3 storage batteries, a converter, and contains no wind generator. The surface of the photovoltaic panels represents 12.7 m^2. The net present cost of this configuration is estimated at 4125 EUR. The second configuration B contains a hybrid photovoltaic/wind system. There are fewer photovoltaic panels than in configuration A and counts 28 panels with a surface of 9.6 m^2 generating a power of 1.4 kW.

The number of storage batteries and converters is the same as in configuration A. Concerning the net present cost of this configuration, it is higher and is estimated at 5735 EUR.

5.2 Production result and electricity consumption

This section shows more details about the two configurations by comparing the energy produced and consumed annually by each configuration (kWh/year). Figures 10 and 11 show the average hourly electricity production for each day of the months of the year in both configurations.

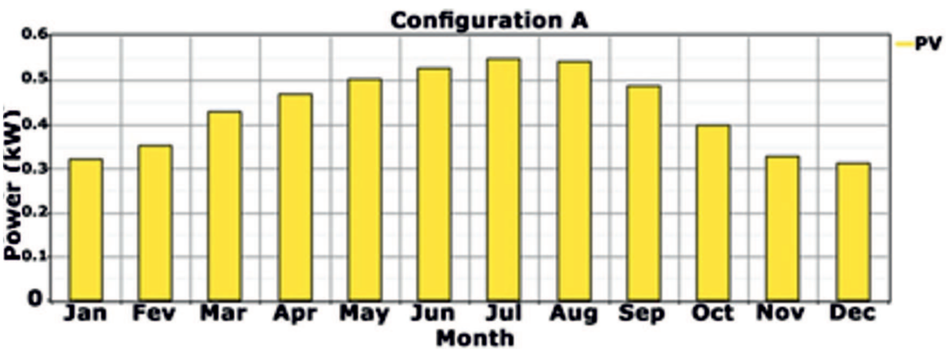

Figure 10: Average hourly electricity production for each day of the month in the configuration A.

According to Fig. 10, it has been found that the production of electrical energy comes only from the photovoltaic system estimated at 3803 kWh/year. The average hourly production is less than 0.4 kW/h from November to February, unlike the other months of the year when this average is greater than or equal to 0.5 kW/h. The electrical energy consumed directly from the AC bus represents 1756 kWh/year, the rest of the energy produced is stored in batteries so that it can be used at night or during the period when there is a lack of solar radiation and represents 1606 kWh/year or 42.2% of the production of the pure photovoltaic system. Figure 11 shows that the production of electric energy from the photovoltaic/wind hybrid system is

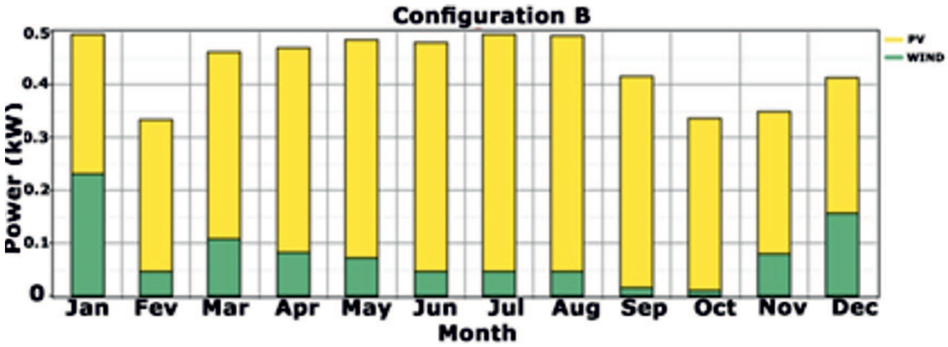

Figure 11: Average hourly electricity production for each day of the months of the configuration B.

estimated at 3822 kWh/year where 82% is generated by photovoltaic panels and 18% by the wind system, i.e., 3132 kWh/year and 690 kWh/year respectively.

The energy generated by the photovoltaic panels is much higher than that of the wind system during all the months of the year. The average hourly production in February, October, and November is less than 0.4 kW/h. The electric energy consumed directly from the AC bus represents 1755 kWh/year, the rest is stored in the batteries in order to be used at night or during the deficit period of the two energy sources and represents 1730 kWh/year or 45.3% of the production of the hybrid system.

5.3 Other results of configuration A

This part will discuss the behaviour of photovoltaic panels with storage during all days of the year. The annual energy produced by the photovoltaic system per day and over the whole year is represented in Fig. 12. As shown in figure the production is stable during all the days of the year and this between 6 am and 7 pm hourly production is around 0.4 kW up to 1.2 kW continuously and can even reach 1.8 kW, and very rarely 2 kW during the day. The operating hours of photovoltaic panels are estimated at 4387 hours per year.

Figure 13 shows the daily charging and discharging status of batteries throughout the year, which shows that the batteries are always almost fulfilled during the year except during the summer period which lasts from June until August when it can reach an estimated depth of discharge of 90% to 65%. In mid-July the battery discharge will reach its maximum of 50%

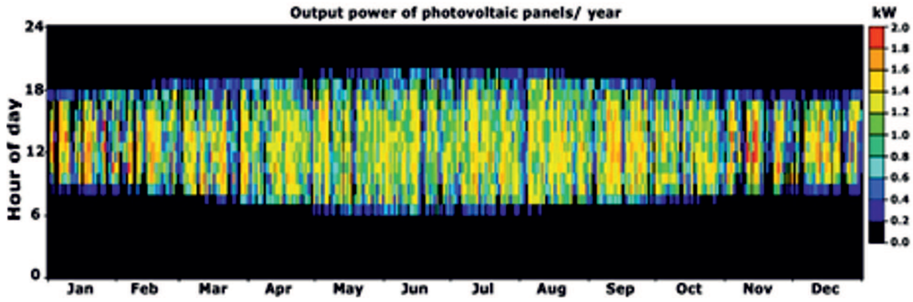

Figure 12: Daily energy produced by PV throughout the year.

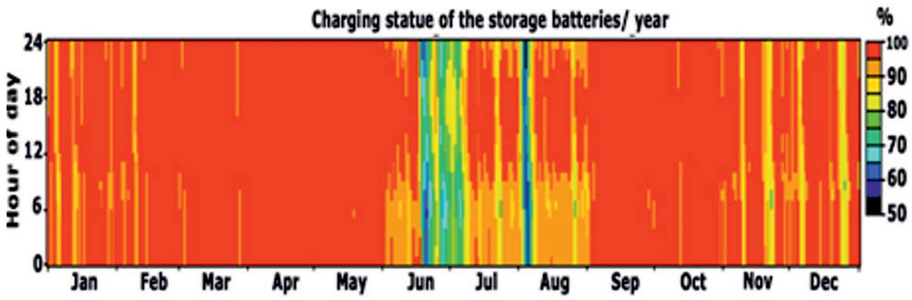

Figure 13: Daily status of charge and discharge of batteries during the year.

for a few hours at night. The energy converter operates fully throughout the year.

5.4 Other results of configuration B

This section will discuss the behavior of the photovoltaic/wind hybrid system during all days of the year. The annual energy produced by the photovoltaic and wind systems each day of the year is shown in Figs. 14 and 15, respectively.

From figures it was noticed that the production of the photovoltaic system is dominant during the year while it is reduced during the months of January, November, and December. This phenomenon is due to the presence of the wind generator which is associated with the photovoltaic system. Nevertheless, the wind production is essentially valid only in the months of December and January. It is estimated very low ranging between 0.14 and 0.72 kW per hour. It reaches its maximum value of 2.23 kW during two hours of production in mid-January. The number of wind turbine operating

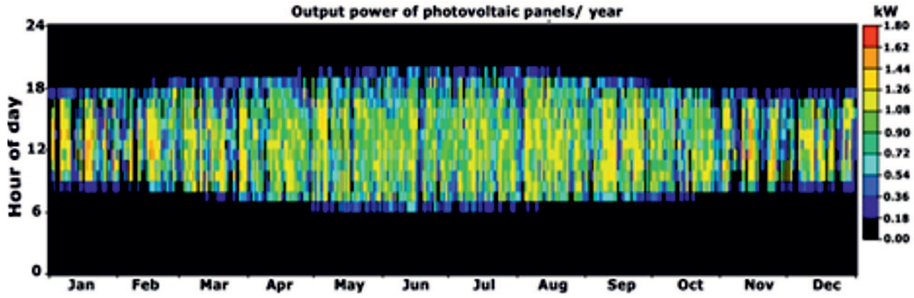

Figure 14: Daily energy produced by PVs during the year.

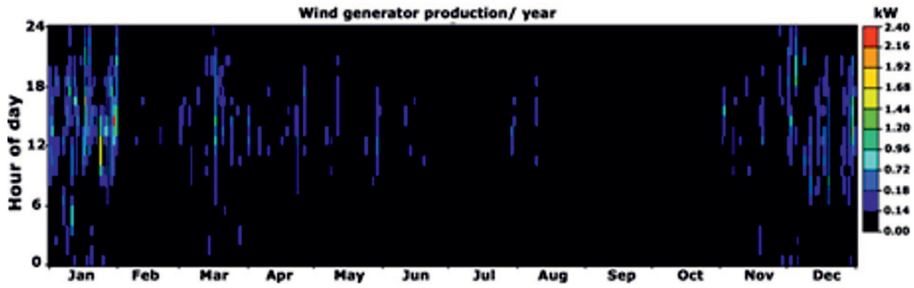

Figure 15: Daily energy produced by wind turbine during the year.

hours is low. The batteries will have the same behavior as in the A configuration and the converter will operate fully during the year. Consequently, the A configuration is better than the B configuration, on account of the total net cost of the investment, which is respectively 4125 EUR against 5735 EUR.

6 Conclusion

This study focused on the use of two sources of energy, namely wind and solar to identify a system of electrical energy production, coupled or separated, based on these two sources, and which aims to develop the electrical energy required daily by a house. The study conducted in this article leads to evaluate the optimal configuration for supplying a continuous availability of electrical energy at any time of the day to a residential apartment autonomous and away from the conventional power network in Tlemcen, Algeria. However, the presented methodology can be used for identifying the optimum energy production system for any location in the world and especially for small power sites.

Based on the results, the following conclusions are drawn:

1. Solar resource assessment for the region shows the possibility of adequate power generation potential from sole photovoltaic systems. The wind resource analysis shows the inefficiency of the wind energy generation due to the very low wind speed of this non windy site. So this region can only be considered for solar power generation as opposed to wind energy.
2. The optimum practicable configurations of electrical power system for energy demand of 3.26 kWh/day in the winter season and 9.15 kWh/day in the summer season are determined.
3. Two configurations that distinguish this study are highlighted, The first is purely photovoltaic and consists of 34 panels, 3 storage batteries and 1 converter with a total cost of 4125 EUR, and the second represents a hybrid photovoltaic/wind system, and consists of 28 panels, 1 wind turbine, 3 storage batteries and 1 converter with a total cost of 5735 Euros.

The main obstacle in the production of energy for hybrid systems is the lack or failure of a source either solar or wind. Hence the latter must be strong and constant for a better energetic profit.

Received 18 May, 2018

References

[1] Ministére de l'Energie et des Mines: *Guide des Energies Renouvelables*, 2007.

[2] Maouedj R.: *Application de l'énergie photovoltaïque au pompage hydraulique sur les sites de Tlemcen et de Bouzaréah.* MSc thesis, Université de Tlemcen, Tlemcen 2005.

[3] Gumuła S., Stanisz K.: *Variants of Technical Solutions of the Demand for Electrical Energy of the Building Energetically Independent.* Scientific Works of the Warsaw University of Technology, ser. Conf. 26, Warszawa 2009.

[4] Saheb-Koussa D, Belhamel M. Benferhat K.: *Contribution à l'étude théorique du comportement d'un systéme hybride (éolien- photovoltaïque-diesel) de production d'électricité sans interruption.* Afrique Science **5**(2009), 1, 23–38.

[5] Reindl D.T., Beckman W.A., Duffie J.A.: *Evaluation of hourly tilted surface radiation models.* Sol. Energy **45**(1990), 1, 9–17.

[6] El Hadidy M.A.: *Performance evaluation of hybrid (wind/solar/diesel) power systems.* Renew. Energ. **2**6(2002), 3, 401–413.

[7] Khahro S.F., Tabbassum K., Soomro A.M., Dong L., Liao X.: *Evaluation of wind power production prospective and Weibull parameter estimation methods for Babaurband, Sindh Pakistan.* Energy Convers. Manage. **78**(2014), 956–967.

[8] Gumuła S., Knap T., Strzelczyk P., Szczerba Z.: *Wind Power Industry.* Wyd. AGH, Krakow 2006.

[9] Akpinar E.K., Akpinar S.: *An assessment on seasonal analysis of wind energy characteristics and wind turbine characteristics.* Energy Convers. Manage. **46**(2005), 1848–1867.

[10] Gumuła S., Woźniak A.: *The influence of power properties of the wind turbine on energetic and economic indicators of electric energy production.* Trans. Inst. Fluid-Flow Mach. **132**(2016), 57–69.

[11] Kolokotsa D. *et al.*: *Methodology for optimal sizing of stand-alone photovoltaic/wind/generator systems using genetic algorithms.* Int. J. Solar Energy **80**(2006, 9, 1072–1088.

[12] Keyhani A., Ghasemi-Varnamkhasti M., Khanali M., Abbaszadeh R.: *An assessment of wind energy potential as a power generation source in the capital of Iran.* Tehran. Energy **35**(2010), 188–201.

[13] Lu Y, Burnett L. *et al.*: *Investigation on wind power potential on Hong Kong islands-an analysis of wind power and wind turbine characteristics.* Int. J. Renew. Energ. **27**(2002), 1, 1–12.

[14] Bogdan S.B., Salameh Z. M.: *Methodology for optimally sizing the combination of a battery bank and PV array in a wind/PV hybrid system.* IEEE Trans. Energy Conversion **11**(1996),2, 367–375.

[15] Bin A, Hongxing Y. *et al.*: *Computer aided design for PV/wind hybrid system.* Int. J. Renew. Energ. **28**(2003), 1491–1512.

[16] Gergaud O.: *Modélisation énergétique et optimisation économique d'un systéme de production éolien et photovoltaique couplé au réseau et associé à un Accumulateur.* PhD thesis, Electrotechnique, Ecole Normale Supérieure de Cachan, 2002.

[17] Protogeropouios C., Brinkworth B.J., Marshall R.H.: *Sizing and techno economical optimization for hybrid solar photovoltaic/wind power systems with battery storage.* Int. J. Energy Res. **21**(1997), 465–479.

[18] Belghitri H.: *Modélisation, simulation et optimisation d'un systéme hybride éolien photovoltaique.* MSc thesis, Université de Tlemcen, Tlemcen 2011.

[19] http://www.bateriehaze.pl/

[20] http://fotoogniwa-sklep.pl/